

# Electron-Deficient Poly(*p*-phenylene vinylene) Provides Electron Mobility over $1 \text{ cm}^2 \text{ V}^{-1} \text{ s}^{-1}$ under Ambient Conditions

Ting Lei,<sup>†</sup> Jin-Hu Dou,<sup>†</sup> Xiao-Yu Cao,<sup>\*,‡</sup> Jie-Yu Wang,<sup>\*,†</sup> and Jian Pei<sup>\*,†</sup>

<sup>†</sup>Beijing National Laboratory for Molecular Sciences, the Key Laboratory of Bioorganic Chemistry and Molecular Engineering of Ministry of Education, College of Chemistry and Molecular Engineering, Peking University, Beijing 100871, China

<sup>‡</sup>College of Chemistry and Chemical Engineering, Xiamen University, Xiamen 361005, China

**S** Supporting Information

**ABSTRACT:** Poly(*p*-phenylene vinylene) derivatives (PPVs) are one of the most widely investigated *p*-type polymers in organic electronics. PPVs generally exhibit electron mobilities lower than  $10^{-4} \text{ cm}^2 \text{ V}^{-1} \text{ s}^{-1}$ , thus hindering their applications in high-performance polymer field-effect transistors and organic photovoltaics. Herein, we design and synthesize a novel electron-deficient PPV derivative, benzodifurandione-based PPV (BDPPV). This new PPV derivative displays high electron mobilities up to  $1.1 \text{ cm}^2 \text{ V}^{-1} \text{ s}^{-1}$  under ambient conditions (4 orders of magnitude higher than those of other PPVs), because it overcomes common defects in PPVs, such as conformational disorder, weak interchain interaction, and a high LUMO level. BDPPV represents the first polymer that can transport electrons over  $1 \text{ cm}^2 \text{ V}^{-1} \text{ s}^{-1}$  under ambient conditions.

Poly(*p*-phenylene vinylene) derivatives (PPVs) are among the earliest and the most widely investigated polymers in organic electronics.<sup>1</sup> As typical *p*-type polymers,<sup>2</sup> PPVs have been used to fabricate the first polymer light-emitting diode (PLED),<sup>3</sup> the first bulk heterojunction (BHJ) solar cell,<sup>4</sup> and the first optically pumped solid-state laser.<sup>5</sup> Considerable efforts have been devoted to improving their emission color, efficiency, and lifetime in PLEDs,<sup>6</sup> as well as power conversion efficiency in solar cells.<sup>7</sup> Nonetheless, PPVs were seldom applied in field-effect transistors (FETs) due to their low hole mobilities ( $10^{-5}$ – $10^{-2} \text{ cm}^2 \text{ V}^{-1} \text{ s}^{-1}$ ).<sup>8</sup> Moreover, their electron mobilities are lower ( $10^{-5}$ – $10^{-4} \text{ cm}^2 \text{ V}^{-1} \text{ s}^{-1}$ ), even when a low-work-function metal (Ca) and a hydroxyl-free gate dielectric were used to fabricate the device and all operations were performed under an inert atmosphere.<sup>9</sup> Hence, one may ask, “can high carrier mobility be achieved in PPV-based polymers?”

Recently, the application of several electron-deficient dyes, such as diketopyrrolopyrrole (DPP),<sup>10</sup> isoindigo (II),<sup>11</sup> naphthalene diimide (NDI),<sup>12</sup> and benzobisthiadiazole (BBT)<sup>13</sup> in polymer FETs afforded high hole mobilities under ambient conditions and high electron mobilities in nitrogen. Nevertheless, high electron mobilities over  $1 \text{ cm}^2 \text{ V}^{-1} \text{ s}^{-1}$  under ambient conditions have not yet been reported, although polymers with high electron mobilities under ambient conditions are important for both fundamentally understanding carrier transport and advancing practical applications. The current scenario of new polymer design mainly focuses on thiophene-based donor–acceptor copolymers (third-generation polymer

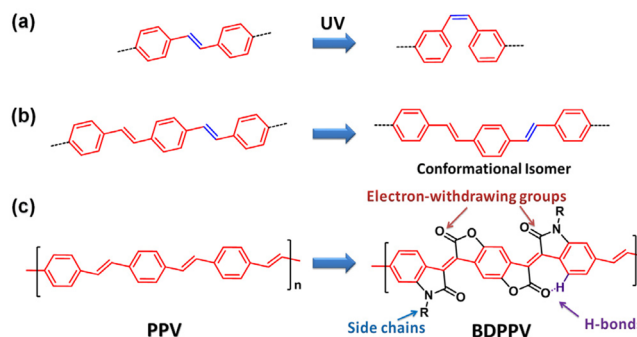


**Figure 1.** (a) Double bond isomerization of the PPV segment under UV irradiation. (b) Conformational isomers in PPV after single bond rotation. (c) Design strategy for the electron-deficient PPV—BDPPV.

named by Heeger), and PPVs (second-generation polymer named by Heeger) are almost neglected.<sup>14</sup>

Carrier mobility in a conjugated polymer is determined by intrachain and interchain transport.<sup>15</sup> Increasing the effective conjugation length and reducing torsional disorder along the polymer backbone improve the intrachain transport.<sup>16</sup> Good  $\pi$ – $\pi$  stacking and ordered polymer packing, on the other hand, increase the interchain transport. Previously, we proved that the backbone curvature of polymers has a significant influence on their carrier mobility, and polymers with linear backbones have mobilities several orders of magnitude higher than those with wave-like backbones.<sup>17</sup> Thus, the low mobility of PPVs is presumably caused by the following:

(1) The double bonds in PPVs readily undergo *trans* to *cis* conformational transformation under UV light both in solution and in solid state (Figure 1a).<sup>18</sup>

(2) Even for all-*trans* backbones, the single bonds in PPVs rotate freely at room temperature, creating many conformational isomers (Figure 1b).

(3) PPVs generally have weak interchain interactions and are amorphous in the solid state,<sup>19</sup> thus resulting in slow interchain carrier transport.

(4) The LUMO levels of PPVs ( $-2.7$  to  $-3.2 \text{ eV}$ )<sup>9</sup> are too high to achieve stable electron transport under ambient conditions.

The first two issues not only limit the intrachain carrier mobilities in PPVs but also weaken the interchain  $\pi$ – $\pi$  interactions, thus further prohibiting the interchain carrier transport.

Received: April 11, 2013

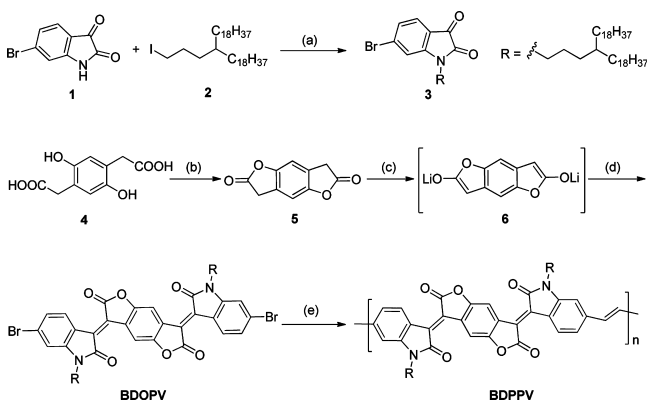
Published: May 15, 2013

Currently, the most effective approach to obtain high electron mobilities in polymers, especially under ambient conditions, is to introduce electron-withdrawing groups to lower their LUMO levels.<sup>20</sup>

Herein, we try to tackle these problems in traditional PPVs by synthesizing a novel PPV derivative, a benzodifurandione-based PPV (**BDPPV**) (Figure 1c). First, strong electron-withdrawing carbonyl groups are introduced on the double bonds of PPV to lower its LUMO level. Second, the carbonyl groups can form intramolecular hydrogen bonds to prevent the conformational transformation of the double bonds, affording a giant “locked” aromatic plane. The enlarged aromatic backbone of **BDPPV** may also contribute to the overlaps of intermolecular frontier orbitals, thus facilitating interchain transport. Third, 4-octadecyldocosyl groups are used as side chains because we have demonstrated that a more distant branching point of side chains can enhance interchain  $\pi$ - $\pi$  stacking and thereby improve carrier mobilities.<sup>21</sup> Using **BDPPV** as an active layer, FETs with electron mobilities up to  $1.1 \text{ cm}^2 \text{ V}^{-1} \text{ s}^{-1}$  are obtained under ambient conditions, 4 orders of magnitude higher than those of other PPVs! To our knowledge, this result is among the highest in *n*-type polymer FETs, and **BDPPV** represents the first polymer that can transport electrons over  $1 \text{ cm}^2 \text{ V}^{-1} \text{ s}^{-1}$  under ambient conditions.<sup>22</sup>

Scheme 1 illustrates the synthetic route to polymer **BDPPV**. The synthesis started from the alkylation of commercially

### Scheme 1. Synthetic Approach to Polymer **BDPPV**<sup>a</sup>



<sup>a</sup>Reagents and conditions: (a)  $\text{K}_2\text{CO}_3$ , THF/DMF,  $50^\circ\text{C}$ , 80%; (b)  $\text{Ac}_2\text{O}$ , toluene,  $100^\circ\text{C}$ , 94%; (c) LTMP, THF,  $-78^\circ\text{C}$ , 30 min; (d) 3, THF,  $0^\circ\text{C}$ , 2 h, two steps, 67%; (e) (*E*)-1,2-bis(tributylstannyl)ethene,  $\text{Pd}_2(\text{dba})_3$ ,  $\text{P}(o\text{-tol})_3$ , chlorobenzene, microwave, 83%.

available 6-bromoisatin (**1**), giving **3** in 80% yield. 2,2'-(2,5-Dihydroxy-1,4-phenylene)diacetic acid (**4**) was synthesized from 1,4-benzoquinone in over 10-g scale.<sup>23</sup> **4** was subjected to a dehydration reaction using acetic anhydride to afford dilactone **5**. Lithium 2,2,6,6-tetramethylpiperidine (LTMP) was used to generate intermediate **6** and react with **3**, providing the desired benzodifurandione-based oligo(*p*-phenylene vinylene) (**BDOPV**) in moderate yield. A Stille coupling polymerization between **BDOPV** and (*E*)-1,2-bis(tributylstannyl)ethene gave polymer **BDPPV** in 83% yield. The molecular weight of **BDPPV** was evaluated by high temperature gel permeation chromatography at  $140^\circ\text{C}$  using 1,2,4-trichlorobenzene as the eluent. The polymer displayed a high molecular weight with an  $M_n$  of 37.6 kDa and a PDI of 2.38. The large PDI of **BDPPV** may be caused by its strong aggregation tendency. The polymer showed

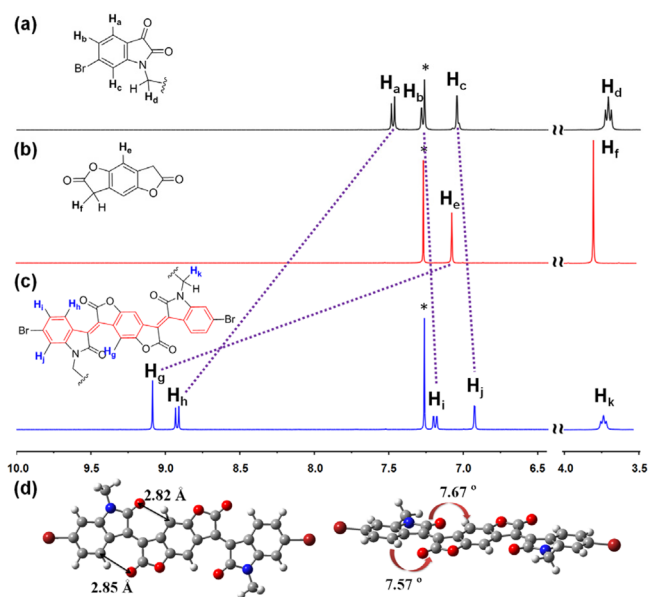


**Figure 2.**  $^1\text{H}$  NMR spectra of (a) **3**, (b) **5**, and (c) **BDOPV** in  $\text{CDCl}_3$  (\*: solvent peak). (d) The optimized molecular structure of **BDOPV** (B3LYP/6-311+G(d,p)).

excellent thermal stability with a decomposition temperature over  $390^\circ\text{C}$ .

Figure 2 compares the  $^1\text{H}$  NMR spectra of compounds **3**, **5**, and **BDOPV**. After the basic condensation reaction, the signal of  $\text{H}_a$  of compound **3** obviously shifted from 7.46 to 8.92 ppm ( $\text{H}_h$  in **BDOPV**). The signal of methylene ( $\text{H}_f$ ) in reactant **5** disappeared, and another signal of  $\text{H}_e$  on the benzene ring significantly shifted from 7.07 to 9.09 ppm ( $\text{H}_a$  in **BDOPV**). The  $^1\text{H}$  NMR spectrum of **BDOPV** clearly displayed four signals in the aromatic region, agreeing well with its chemical structure and chemical environment. The optimized structure of **BDOPV** displayed an almost planar backbone with small dihedral angles of  $\sim 7.6^\circ$  (Figure 2d). The C-H<sub>a</sub>-O and C-H<sub>b</sub>-O angles are approximately linear, and the C-O bond distances (ca. 2.8 Å) are shorter than the combined van der Waals radii (3.3 Å).<sup>24</sup> These results indicate that four intramolecular hydrogen bonds are formed,<sup>25</sup> which may contribute to the planarity and shape persistency of **BDOPV**.

Under UV light irradiation (365 nm), the double bonds in PPVs usually undergo a *trans* to *cis* conformational change.<sup>18</sup> Figure S3 displays the spectral change of a commercially available model compound 1,4-bis((*E*)-2-methylstyryl)benzene under UV irradiation. Clearly, the compound showed decreased long-wavelength and increased short-wavelength absorption, indicating a conformational change from *trans* to *cis* occurred under UV irradiation. In contrast, **BDOPV** showed no spectral change under UV or visible light irradiation, which may be largely due to its “locked skeleton”. More importantly, both the solution and the film of polymer **BDPPV** showed excellent stability under UV or visible light exposure. Although one-third of the double bonds in **BDPPV** are not locked by intramolecular hydrogen bonds, a conformational change in **BDPPV** was not observed. This phenomenon might be attributed to the largely conjugated **BDOPV** core, which has a strong tendency to undergo intermolecular stacking, thus creating a large steric hindrance to prevent the double bond from adopting a *cis*-conformation in **BDPPV**.

The absorption spectra of **BDOPV** in solution and polymer **BDPPV** in solution, thin film, and annealed film are shown in

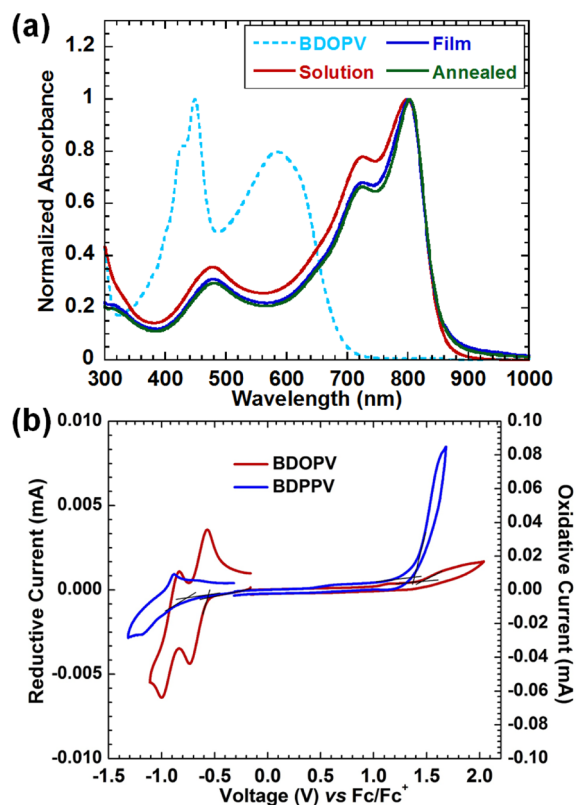


**Figure 3.** (a) Normalized absorption spectra of **BDOPV** in  $\text{CHCl}_3$  ( $10^{-5}$  M, dashed line) and **BDPPV** in  $\text{CHCl}_3$  ( $10^{-5}$  M), in film and in annealed film. (b) Cyclic voltammograms of **BDOPV** in DCB solution (5 mg/mL) and **BDPPV** in drop-casted film.

Figure 3. **BDOPV** displays two absorption peaks with an onset at 700 nm and a band gap of 1.80 eV. After polymerization, the new double bond in **BDPPV** further extends the conjugation length, leading to strong near-infrared absorption with a band gap of 1.42 eV. The main absorption peak of **BDPPV** in film only showed minimal red shift compared to those in solution, and an obvious increase of the intensity of 0–0 vibrational peak was observed. Annealing the film led to a further increase in intensity of the 0–0 peak. These results indicate that the polymer backbone became more planar in film and annealing was helpful for further adjustment. For conjugated polymers, intermolecular stacking and conformational change may significantly shift the absorption spectra,<sup>26</sup> which is common for most PPVs.<sup>19</sup> However, no significant change was observed for **BDPPV** from solution to film. The absence of bathochromic effects indicates that the polymers probably formed some preaggregates in solution due to strong intermolecular interactions.<sup>27</sup> In cyclic voltammetry (CV) measurements, **BDOPV** displayed low HOMO/LUMO levels of  $-6.21/-4.24$  eV. Compared with the HOMO/LUMO levels of PPV ( $-5.2/-2.7$  eV),<sup>9</sup> **BDPPV** exhibited significantly lowered HOMO/LUMO levels ( $-6.12/-4.10$  eV), which is also consistent with the HOMO/LUMO levels ( $-5.83/-4.41$  eV) estimated from the photoelectron spectroscopy (Figure S4) and optical band gap. Note that this LUMO level is also lower than those of several ambient-stable *n*-type polymers, including NDI and PDI based polymers.<sup>28</sup> Computational analysis of the oligomer of **BDPPV** showed that the HOMO and LUMO are well delocalized along the polymer backbone, and the HOMO and LUMO distributions of **BDPPV** are similar to those of PPV, due to their identical alternative phenylene vinylene skeletons (Figure S5).

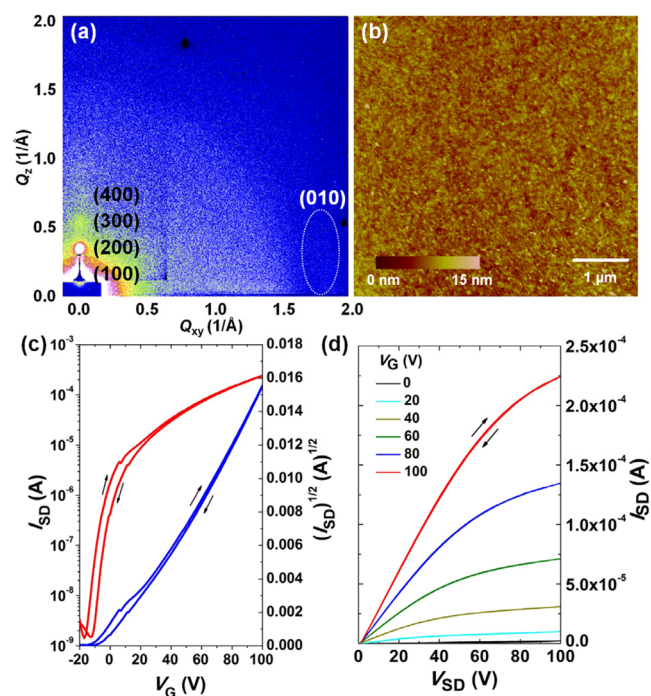


**Figure 4.** (a) 2D-GIXD pattern and (b) AFM height images of polymer **BDPPV** film prepared by spin-coating its DCB solution (3 mg/mL); (c) Transfer and (d) output characteristics of a **BDPPV** device under ambient conditions ( $L = 10 \mu\text{m}$ ,  $W = 200 \mu\text{m}$ ,  $C_i = 3.7 \text{ nF cm}^{-2}$ ), measured  $V_T = 5$  V.

PPVs generally form amorphous films with weak X-ray scattering, due to their weak interchain interactions and disordered packing.<sup>19</sup> To investigate the molecular packing of **BDPPV** in thin film, grazing-incident X-ray diffraction (GIXD) and tapping-mode atomic force microscopy (AFM) were used (Figure 4a and 4b). The polymer film of **BDPPV** showed a strong out-of-plane diffraction peak (100) at  $2\theta = 2.20^\circ$ , corresponding to a *d*-spacing of 32.3 Å ( $\lambda = 1.24$  Å). Another three diffraction peaks corresponding to (*h*00) were also observed, suggesting that a good lamellar edge-on packing was formed in the film. An in-plane (010) peak attributed to the interchain  $\pi$ - $\pi$  stacking was also observed with a distance of 3.55 Å, comparable to those of other semiconducting polymers. The AFM height image of **BDPPV** showed crystalline fiber-like intercalating networks with a root-mean-square (RMS) deviation of 1.30 nm. Such crystalline networks are presumably caused by strong interchain interactions. Unlike other PPVs, **BDPPV** clearly showed a much stronger aggregation tendency and more ordered packing. Thus, better interchain carrier transport is expected.

The low-lying LUMO of **BDPPV** indicates that it could be suitable for ambient-stable electron transport. A top-gate/bottom-contact (TG/BC) device configuration was used to fabricate polymer FETs, because this device configuration has better injection characteristics and encapsulation effects.<sup>29</sup> The semiconducting layer was deposited by spin-coating a polymer solution (3 mg/mL in 1,2-dichlorobenzene, DCB) on a patterned Au/SiO<sub>2</sub>/Si substrate. After thermal annealing of the film for 10 min, a CYTOP solution was spin-coated as the dielectric layer, and an aluminum layer was thermally evaporated as the gate electrode. FET devices of **BDPPV** clearly showed *n*-type transport characteristics under ambient conditions (Figure 4c and 4d). Several annealing temperatures were tried, and annealing at 200 °C gave the best device performance. The polymer showed the highest

electron mobilities up to  $1.1 \text{ cm}^2 \text{ V}^{-1} \text{ s}^{-1}$  with an average mobility of  $0.84 \text{ cm}^2 \text{ V}^{-1} \text{ s}^{-1}$ . This result represents the first polymer FET that can transport electrons over  $1 \text{ cm}^2 \text{ V}^{-1} \text{ s}^{-1}$  under ambient conditions. Note that the transfer and output characteristics showed negligible hysteresis at high gate voltages, indicating that there are only a few traps for electrons, presumably due to the significantly lowered LUMO level. No contact resistance is observed in output curves, indicating the ohmic contact between the polymer and gold electrode. Furthermore, time-dependent decay of the BDPPV device was also performed by storing the devices under room light and ambient conditions. The device could function effectively after being stored for 30 days, affording an electron mobility of  $0.31 \text{ cm}^2 \text{ V}^{-1} \text{ s}^{-1}$  (Figure S7), comparable to those of other high-performance *n*-type polymer FETs.<sup>22</sup> The slow degradation of the device was probably caused by the further diffusion of oxygen and water into the film.<sup>30</sup> However, we believe that polymers with lower LUMO levels may have better device performance and stability.

In conclusion, we have demonstrated that molecular engineering of the PPV skeleton can overcome factors that limit electron mobility in PPVs, such as conformational disorder, weak interchain interactions, and high LUMO levels. The novel designed electron-deficient PPV derivative “locked” the polymer backbone by intramolecular hydrogen bonds, endowing itself with excellent UV and visible light stability, a stronger aggregation tendency, better crystallinity, a lower LUMO level, and above all higher electron mobilities up to  $1.1 \text{ cm}^2 \text{ V}^{-1} \text{ s}^{-1}$  under ambient conditions. Furthermore, FET devices based on BDPPV also showed good ambient stability for at least 30 days. Our molecular engineering strategy effectively avoids the defects of other PPVs and increases the electron mobility of PPVs from  $10^{-4} \text{ cm}^2 \text{ V}^{-1} \text{ s}^{-1}$  to over  $1 \text{ cm}^2 \text{ V}^{-1} \text{ s}^{-1}$ , which may trigger the renaissance of the second-generation polymer. Through further molecular modulation, the electron-deficient BDOPV and its derivatives could find broad applications for organic electronics requiring efficient electron transport, such as ambipolar FETs and acceptors in organic solar cells.

## ■ ASSOCIATED CONTENT

### Supporting Information

Experimental details and characterization data. This material is available free of charge via the Internet at <http://pubs.acs.org>.

## ■ AUTHOR INFORMATION

### Corresponding Author

[jianpei@pku.edu.cn](mailto:jianpei@pku.edu.cn); [xcao@xmu.edu.cn](mailto:xcao@xmu.edu.cn); [jiyewang@pku.edu.cn](mailto:jiyewang@pku.edu.cn)

### Notes

The authors declare no competing financial interests.

## ■ ACKNOWLEDGMENTS

This work was supported by the Major State Basic Research Development Program (Nos. 2009CB623601 and 2013CB933501) from the Ministry of Science and Technology, and National Natural Science Foundation of China. The authors thank beamline BL14B1 (Shanghai Synchrotron Radiation Facility) for providing the beam time.

## ■ REFERENCES

- (1) Kraft, A.; Grimsdale, A. C.; Holmes, A. B. *Angew. Chem., Int. Ed.* **1998**, *37*, 402. (b) Beaujuge, P. M.; Fréchet, J. M. J. *J. Am. Chem. Soc.* **2011**, *133*, 20009.
- (2) (a) Meijer, E. J.; de Leeuw, D. M.; Setayesh, S.; van Veenendaal, E.; Huisman, B. H.; Blom, P. W. M.; Hummelen, J. C.; Scherf, U.; Klapwijk,

T. M. *Nat. Mater.* **2003**, *2*, 678. (b) Blom, P. W. M.; de Jong, M. J. M.; van Munster, M. G. *Phys. Rev. B* **1997**, *55*, R656.

(3) Burroughes, J. H.; Bradley, D. D. C.; Brown, A. R.; Marks, R. N.; Mackay, K.; Friend, R. H.; Burns, P. L.; Holmes, A. B. *Nature* **1990**, *347*, 539.

(4) Yu, G.; Gao, J.; Hummelen, J. C.; Wudl, F.; Heeger, A. J. *Science* **1995**, *270*, 1789.

(5) (a) Hide, F.; Díaz-García, M. A.; Schwartz, B. J.; Andersson, M. R.; Pei, Q.; Heeger, A. J. *Science* **1996**, *273*, 1833. (b) Tessler, N.; Denton, G. J.; Friend, R. H. *Nature* **1996**, *382*, 695.

(6) (a) Welter, S.; Brunner, K.; Hofstra, J. W.; De Cola, L. *Nature* **2003**, *421*, 54. (b) Akcelrud, L. *Prog. Polym. Sci.* **2003**, *28*, 875.

(7) (a) Chen, J.; Cao, Y. *Acc. Chem. Res.* **2009**, *42*, 1709. (b) Wang, L.; Liu, Y.; Jiang, X.; Qin, D.; Cao, Y. *J. Phys. Chem. C* **2007**, *111*, 9538.

(8) (a) Wang, C.; Dong, H.; Hu, W.; Liu, Y.; Zhu, D. *Chem. Rev.* **2011**, *112*, 2208. (b) van Breemen, A. J. J. M.; Herwig, P. T.; Chlon, C. H. T.; Sweelssen, J.; Schoo, H. F. M.; Benito, E. M.; de Leeuw, D. M.; Tanase, C.; Wildeman, J.; Blom, P. W. M. *Adv. Funct. Mater.* **2005**, *15*, 872.

(9) Chua, L.-L.; Zaumseil, J.; Chang, J.-F.; Ou, E. C. W.; Ho, P. K. H.; Siringhaus, H.; Friend, R. H. *Nature* **2005**, *434*, 194.

(10) (a) Li, J.; Zhao, Y.; Tan, H. S.; Guo, Y.; Di, C.-A.; Yu, G.; Liu, Y.; Lin, M.; Lim, S. H.; Zhou, Y.; Su, H.; Ong, B. S. *Sci. Rep.* **2012**, *2*, 754. (b) Nielsen, C. B.; Turbiez, M.; McCulloch, I. *Adv. Mater.* **2013**, *25*, 1859. (c) Chen, H.; Guo, Y.; Yu, G.; Zhao, Y.; Zhang, J.; Gao, D.; Liu, H.; Liu, Y. *Adv. Mater.* **2012**, *24*, 4618.

(11) (a) Lei, T.; Cao, Y.; Fan, Y.; Liu, C.-J.; Yuan, S.-C.; Pei, J. *J. Am. Chem. Soc.* **2011**, *133*, 6099. (b) Mei, J.; Kim, D. H.; Ayzner, A. L.; Toney, M. F.; Bao, Z. *J. Am. Chem. Soc.* **2011**, *133*, 20130.

(12) Zhan, X.; Facchetti, A.; Barlow, S.; Marks, T. J.; Ratner, M. A.; Wasielewski, M. R.; Marder, S. R. *Adv. Mater.* **2011**, *23*, 268.

(13) (a) Fan, J.; Yuen, J. D.; Cui, W.; Seifert, J.; Mohebbi, A. R.; Wang, M.; Zhou, H.; Heeger, A.; Wudl, F. *Adv. Mater.* **2012**, *24*, 6164. (b) Yuen, J. D.; Fan, J.; Seifert, J.; Lim, B.; Hufschmid, R.; Heeger, A. J.; Wudl, F. *J. Am. Chem. Soc.* **2011**, *133*, 20799.

(14) (a) Heeger, A. J. *Chem. Soc. Rev.* **2010**, *39*, 2354. (b) Yuen, J. D.; Wudl, F. *Energy Environ. Sci.* **2013**, *6*, 392.

(15) Coropceanu, V.; Cornil, J.; da Silva Filho, D. A.; Olivier, Y.; Silbey, R.; Brédas, J.-L. *Chem. Rev.* **2007**, *107*, 926.

(16) Prins, P.; Grozema, F. C.; Schins, J. M.; Patil, S.; Scherf, U.; Siebbeles, L. D. A. *Phys. Rev. Lett.* **2006**, *96*, 146601.

(17) (a) Lei, T.; Cao, Y.; Zhou, X.; Peng, Y.; Bian, J.; Pei, J. *Chem. Mater.* **2012**, *24*, 1762. (b) Osaka, I.; Abe, T.; Shinamura, S.; Takimiya, K. *J. Am. Chem. Soc.* **2011**, *133*, 6852.

(18) (a) Wakioka, M.; Ikegami, M.; Ozawa, F. *Macromolecules* **2010**, *43*, 6980. (b) Moslin, R. M.; Espino, C. G.; Swager, T. M. *Macromolecules* **2008**, *42*, 452.

(19) (a) Chen, S. H.; Su, A. C.; Huang, Y. F.; Su, C. H.; Peng, G. Y.; Chen, S. A. *Macromolecules* **2002**, *35*, 4229. (b) Chen, S. H.; Su, A. C.; Han, S. R.; Chen, S. A.; Lee, Y. Z. *Macromolecules* **2003**, *37*, 181.

(20) (a) Lei, T.; Dou, J.-H.; Ma, Z.-J.; Yao, C.-H.; Liu, C.-J.; Wang, J.-Y.; Pei, J. *J. Am. Chem. Soc.* **2012**, *134*, 20025. (b) Lei, T.; Dou, J.-H.; Ma, Z.-J.; Liu, C.; Wang, J.-Y.; Pei, J. *Chem. Sci.* **2013**, *4*, 2447.

(21) Lei, T.; Dou, J.-H.; Pei, J. *Adv. Mater.* **2012**, *24*, 6457.

(22) Yan, H.; Chen, Z.; Zheng, Y.; Newman, C.; Quinn, J. R.; Dotz, F.; Kastler, M.; Facchetti, A. *Nature* **2009**, *457*, 679.

(23) Wood, J. H.; Cox, L. *Org. Synth.* **1946**, *26*, 24.

(24) Rowland, R. S.; Taylor, R. *J. Phys. Chem.* **1996**, *100*, 7384.

(25) Musah, R. A.; Jensen, G. M.; Rosenfeld, R. J.; McRee, D. E.; Goodin, D. B.; Bunte, S. W. *J. Am. Chem. Soc.* **1997**, *119*, 9083.

(26) Kim, J.; Swager, T. M. *Nature* **2001**, *411*, 1030.

(27) Zhou, N.; Guo, X.; Ortiz, R. P.; Li, S.; Zhang, S.; Chang, R. P. H.; Facchetti, A.; Marks, T. J. *Adv. Mater.* **2012**, *24*, 2242.

(28) Chen, Z.; Zheng, Y.; Yan, H.; Facchetti, A. *J. Am. Chem. Soc.* **2009**, *131*, 8.

(29) (a) Di, C.-A.; Liu, Y.; Yu, G.; Zhu, D. *Acc. Chem. Res.* **2009**, *42*, 1573. (b) Usta, H.; Newman, C.; Chen, Z.; Facchetti, A. *Adv. Mater.* **2012**, *24*, 3678.

(30) Di Pietro, R.; Fazzi, D.; Kehoe, T. B.; Siringhaus, H. *J. Am. Chem. Soc.* **2012**, *134*, 14877.